Slow conversion of the ideal MHD perturbations into a tearing mode after a sawtooth crash

V. Igochine[1], A. Gude[1], S. Günter[1], K. Lackner[1], Q. Yu[1], L. Barrera Orte[1], A. Bogomolov[2], I. Classen[2], R. M. McDermott[1] , N. C. Luhmann, Jr.[3] and ASDEX Upgrade team

[1]*Max Planck Institute for Plasma Physics, Boltzmannstr. 2, 85748 Garching, Germany*
[2]*FOM-Institute DIFFER, Dutch Institute for Fundamental Energy Research, 3430 BE Nieuwegein, The Netherlands*
[3]*University of California at Davis, Davis, California, CA 95616 USA-Institute*

Introduction

Optimization of the plasma performance with respect to beta normalized, β_N , is one of the main goals of fusion research. The expected fusion power scales as β_N^2 and thus even a small increase of this parameter leads to a beneficial effect on the fusion performance. Unfortunately, β_N in standard H-mode and advanced scenario discharges are limited by resistive instabilities, usually neoclassical tearing modes (NTMs). These modes are metastable and can be triggered by other MHD events even at low β_N. Sawtooth crashes provide the strongest internal magnetic perturbations and are able to trigger tearing modes at the smallest β_N values [1,2]. The tearing mode formation process implies magnetic reconnection at the resonant surface, which rearranges magnetic topology. The tearing mode can start either from noise perturbations if the gradient of the plasma current at the resonant surface provides the drive [3], or it requires a trigger event. The second situation is more common for NTMs, which require a seed island to grow. In this paper, the mechanism of the seed island formation by strong internal drive due to sawteeth is investigated in detail. This type of tearing mode formation is considered to be one of the most dangerous for a future fusion reactor like ITER [4] and provides the main motivation for sawtooth control.

Experimental observation of tearing mode formation triggered by a sawtooth crash

In this paper, a combination of all main MHD diagnostics installed in ASDEX Upgrade is used to investigate the triggering process. These are: (i) two independent electron cyclotron emission diagnostics (ECE-Imaging [5] and standard ECE), (ii) magnetic coils and (iii) soft X-ray cameras. The ECE-Imaging diagnostic measures the local electron temperature, T_e, along 14 radial lines of sight with a radial resolution of 1.3 cm. The measurements span the region around the q=2 resonant surface. Standard ECE provides local measurements along a single line of sight which crosses the q=1 and q=2 resonant surfaces. Both diagnostics give information about local temperature perturbations inside the plasma, which depend on the temperature gradient ($\delta T_e = \xi \cdot \nabla \langle T_e \rangle$, where ξ is the displacement). In the case of flat T_e profiles, temperature fluctuations are not visible. Thus, it is difficult to determine the perturbation amplitude from ECE measurements during a phase with strong evolution of the background temperature profile, which is the case directly after a sawtooth crash. Contrary to the ECE diagnostic, magnetic coils located

outside the plasma are able to detect mode perturbations also in this case and provide a good mode amplitude indicator. The measured magnetic signal, Fourier filtered at the mode frequency, represents the total mode amplitude.

Rotation of an MHD mode with respect to the ECE measurement positions is used here to distinguish between kink and tearing modes. The idea is shown schematically in figure 1a. The measurement points 1 and 2 move along the dashed line during mode rotation. In this case, a perturbation caused by an ideal mode produces sinusoidal temperature variations in all channels around the resonant surface, and all these perturbations are in phase. The situation is different for an island structure, where the temperature inside the island is either flat or has an additional maximum (hot island case). In this case, the ECE signal is either flat within the island region or has an additional maximum. This feature gives a direct indication of the island separatrix position and the character of the mode (kink or tearing). This method of the island identification avoids any further assumptions and allows identifying kink-tearing conversion directly. The temporal evolution of experimental ECE signals is shown in figure 1b for discharge 27257. The island structure is clearly visible in all ECE-Imaging channels from 7 to 2 at the end of the time window (t=2.782s). The saturated island width is thus about 6.4 cm. Backward tracing in time allows to identify the point in time at which this feature appears for the first time in each of the channels (indicated by the dashed lines). All ECE signals are in phase before t=2.777s, which is a clear signature of an ideal kink mode. It should be noted that the amplitude of this ideal (2,1) mode is large immediately after the sawtooth crash (t=2.775), as can be seen from magnetic measurements in the bottom time trace of figure 1b.

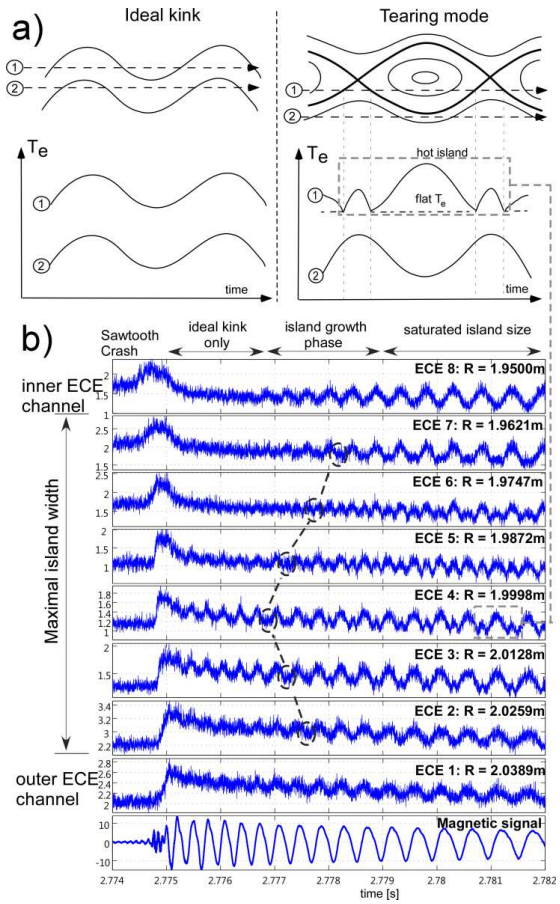

Figure 1. Identification of the island size from local ECE-Imaging measurements. a) Schematic representation of the temperature perturbation for the ideal kink case, island with flat temperature inside and hot island case. b) Direct identification of the transition from ideal kink mode into hot island in different ECE channels for discharge 27257 at t=2.77s. The bottom time trace is the magnetic signal $(d\tilde{B}/dt)$.

The same transition type is observed in the second case (#27257, t=2.5s), but the mode conversion time is much longer for this crash.

The mode amplitude, $A_{(2,1)}$ is extracted from magnetic measurement as $A_{(2,1)} \sim \sqrt{\tilde{B}_{(2,1)}}$, where $\tilde{B}_{(2,1)}$ is the measured perturbation amplitude at the (2,1) frequency. Figures 2a and b show the evolution of the magnetic mode amplitude in comparison with the island size from ECE. The sawtooth crash generates the ideal (2,1) mode directly after the crash. In figure 2a, the mode keeps its ideal character for about $2 \cdot 10^{-3} s$ and only then transforms into an island structure

during $10^{-3}s$. In figure 2b the transition from ideal to tearing mode takes even longer. These time scales are much longer than the sawtooth crash time (about $10^{-4}s$ or less). It is interesting that the mode amplitude of the ideal mode directly after the crash differs almost a factor of two in these two cases and is larger for the fast conversion case. The crash time itself, measured from fast ECE signals, is approximately the same in both cases.

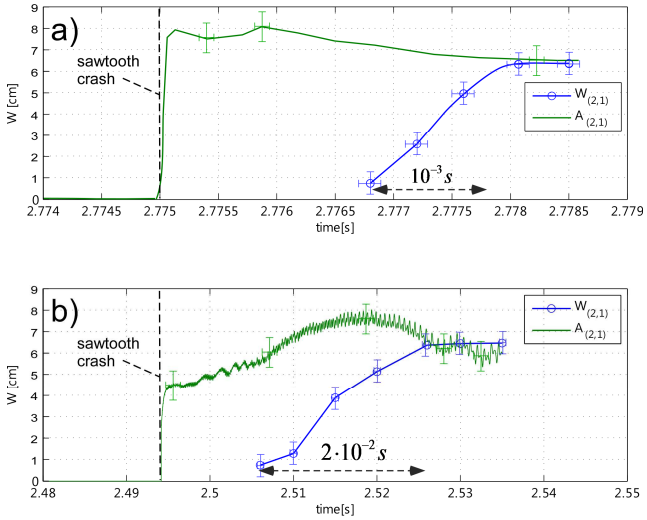

Figure 2. Comparison of the perturbations amplitude for (2,1) mode from magnetic signal, $A_{(2,1)}$, and ECE-Imaging measurements, $W_{(2,1)}$, for two different cases: a) #27257, t=2.77s, the same case as in figure 1; b) #27257, t=2.5s. The mode amplitude from the magnetic signal is scaled to fit the island size from ECE at a later time point, when the saturated island size is reached. The error bars depend on the measurements resolution and mode rotation frequency.

The plasma rotation profiles are almost identical in these two cases, which excludes any influence of the rotation profile on the mode conversion time in these two cases. The same is true for kinetic profiles. The saturated island width, $W_{(2,1),sat} = 6.4[cm]$, is also the same for both cases, which is an indirect indication of similar plasma conditions. Thus, the difference in the time scale of the mode conversion and in the delay of the tearing mode is probably connected to the different drives (different amplitudes of the ideal modes) after the sawtooth crash. The resistive diffusion time required for an 6cm island formation is: $\tau_R = \mu_0 L^2/\eta \approx 0.23s$, where the characteristic length is the saturated island size $L \approx 6cm$, and $\eta \approx 2\cdot 10^{-8}\Omega\cdot m$ is the plasma resistivity at the rational surface. This time is much longer than the observed mode conversion times and shows the inapplicability of the single fluid reconnection picture as expected for collisionless fusion plasmas. This is also confirmed by comparison of characteristic lengths. Experimental plasma parameters at the (2,1) resonant surface show the ion-sound Larmor radius, $\rho_s = c_s/\Omega_i = 8.2\cdot 10^{-3}m$, exceeds the width of the Sweet-Parker layer, $\delta_{sp} = L/\sqrt{S} \approx 1.2\cdot 10^{-5}m$. Nonlinear two-fluid modelling of the NTM formation is discussed below.)

It is important to note that previous observations from other tokamaks, for example from JET [6] or TCV[7], report large island width directly after the crash based on analysis of magnetic or SXR measurements. These measurements also show large amplitude of the mode directly after sawtooth in our cases (A_{tot} in figure 2), but they are not able to distinguish between kink and tearing modes.

A very important question is the origin of the ideal mode at the q=2 resonant surface after the sawtooth crash and its presence long after the crash. Spectral analysis of the signals from the standard ECE diagnostic show temperature perturbations from (2,1)

simultaneously inside the q=1 surface and at the q=2 resonant surface, which indicate the strong coupling between the surfaces. The detected pre-cursor is a (3,3) mode for the case in figure 2b. In this case, the (1,1) frequency is 1/3 of the precursor frequency (18 kHz) and is above the (2,1) mode frequency after the crash (4.5 kHz). The second case in figure 2a has an n=2 precursor with 9kHz, which is approximately twice the frequency of the following (2,1) mode (4kHz). Although the precursors in both cases are not strictly the usual (1,1) mode, one can assume that the crash can leave a residual (1,1) island as post-cursor. Thus, a possible explanation is a strong resistive (1,1) post-cursor, which drives the toroidally coupled ideal (2,1) mode and keeps its amplitude at a relatively large value for a long time after the sawtooth crash. Analysis of the plasma rotation velocity supports the resistive (1,1) post-cursor idea, because the (2,1) mode rotates faster than the plasma at the q=2 surface (2.6kHz-2.9kHz). The presence of sawtooth post-cursors is typical for ASDEX Upgrade [8].

A cylindrical, two fluids, non-linear MHD code is used to simulate the mode triggering [9]. Simulations use the experimental plasma parameters measured by a set of different diagnostics in ASDEX Upgrade. The triggering process is simulated by a variation of the helical flux with (2,1) helicity at the plasma surface. The latter is different from the experimental situation where the perturbation source is at the q=1 surface, but this formulation of the problem simplifies the analysis and excludes the need to model the sawtooth crash dynamic, which is a challenging task by itself. The perturbed flux is set to grow exponentially up to a saturated value on a very short time scale $\left(t_{growth} = 5 \cdot 10^{-5} s\right)$, comparable to the sawtooth crash time. After this time, the amplitude of the external (2,1) perturbation remains constant, which simulates the presence of the perturbation after the crash in the experiment. Results of simulations for different amplitudes of the external perturbations are shown in figure 3. The important result of the calculations is that the conversion time is always longer compared to the typical sawtooth crash time.

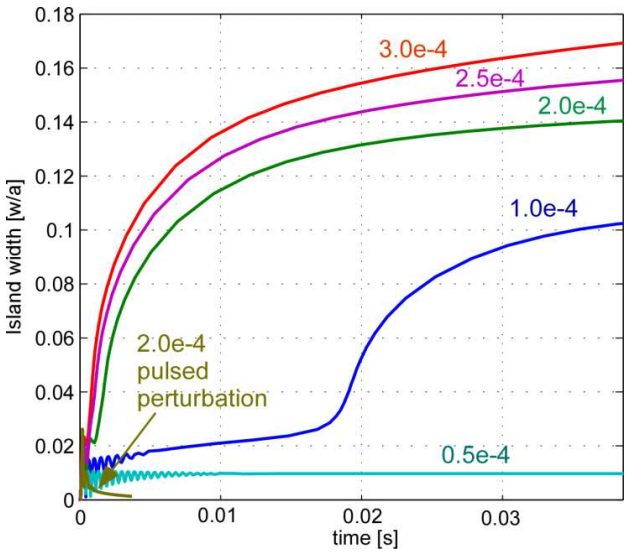

Figure 3. Results of two fluid non-linear MHD simulations are shown. Evolution of the island width in the case of different amplitudes of the perturbed flux at the plasma boundary $\psi_{(2,1)} = 5 \cdot 10^{-5}; 10^{-4}; 2 \cdot 10^{-5}; 2.5 \cdot 10^{-5}; 3 \cdot 10^{-5}$. Special case with pulsed perturbation is shown for $\psi_{(2,1)} = 2 \cdot 10^{-5}$.

This work was partially funded by the Max-Planck/Princeton Center for Plasma Physics. This project has received funding from the Euratom research and training programme 2014-2018.

References

[1] A.Gude, et.al. Nuclear Fusion, Vol.39 (1999), page 127 [2] S. Fietz et.al. Pl. Phys. Contr. Fus. 55 (2013) 085010 [3] H.P.Furth, et.al., Phys. Fluids, (1973), 1054 [4] T.C.Hender et.al. Nucl.Fusion 47 (2007) S128 [5] I. G. J. Classen et.al. Rev. Sci.Instr.81,10D929 (2010) [6] O. Sauter et.al. Phys. Rev. Lett. 88 (2002) 105001 [7] G.P.Canal et.al. Nucl. Fusion 53 (2013) 113026 [8] V.Igochine, et.al. Phys. Plasmas 17, 122506 (2010) [9] Q. Yu et.al. Nucl. Fusion52(2012) 063020